Eur Biophys J
DOI 10.1007/s00249-011-0781-5

ORIGINAL PAPER

EBSA
Biophysics in Europe

Single-channel measurements of an *N*-acetylneuraminic acid-inducible outer membrane channel in *Escherichia coli*

Janhavi Giri · John M. Tang · Christophe Wirth · Caroline M. Peneff · Bob Eisenberg

Received: 11 August 2011 / Revised: 23 November 2011 / Accepted: 6 December 2011

Abstract NanC is an *Escherichia coli* outer membrane protein involved in sialic acid (Neu5Ac, i.e., *N*-acetylneuraminic acid) uptake. Expression of the NanC gene is induced and controlled by Neu5Ac. The transport mechanism of Neu5Ac is not known. The structure of NanC was recently solved (PDB code: 2WJQ) and includes a unique arrangement of positively charged (basic) side chains consistent with a role in acidic sugar transport. However, initial functional measurements of NanC failed to find its role in the transport of sialic acids, perhaps because of the ionic conditions used in the experiments. We show here that the ionic conditions generally preferred for measuring the function of outer-membrane porins are not appropriate for NanC. Single channels of NanC at pH 7.0 have: (1) conductance 100 pS to 800 pS in 100 mM KCl to 3 M KCl), (2) anion over cation selectivity ($V_{reversal} = +16$ mV in 250 mM KCl ‖ 1 M KCl), and (3) two forms of voltage-dependent gating (channel closures above ±200 mV). Single-channel conductance decreases by 50% when HEPES concentration is increased from 100 μM to 100 mM in 250 mM KCl at pH 7.4, consistent with the two HEPES binding sites observed in the crystal structure. Studying alternative buffers, we find that phosphate interferes with the channel conductance. Single-channel conductance decreases by 19% when phosphate concentration is increased from 0 mM to 5 mM in 250 mM KCl at pH 8.0. Surprisingly, TRIS in the baths reacts with Ag|AgCl electrodes, producing artifacts even when the electrodes are on the far side of agar–KCl bridges. A suitable baseline solution for NanC is 250 mM KCl adjusted to pH 7.0 without buffer.

Keywords NanC · Single channel · *E. coli* outer membrane protein · Sialic acid · *N*-acetylneuraminic acid

Introduction

The cell envelope of the Gram negative bacterium *Escherichia coli* acts as a shield that enables the bacteria to survive in drastic environmental conditions as it passes through the human gastrointestinal tract: pH ~1 in the stomach, digestion by enzymes in the small intestine, dehydration in the large intestine, and complete drying after defecation. The cell envelope has two membrane layers separated by the periplasmic space. The outer membrane serves as a selective barrier through which specific solutes (mainly nutrients) can enter the cell. The selective barrier involves channel-forming β-barrel proteins typically called "porins" (Nakae 1976). Porins act as molecular filters that allow passive diffusion of solutes (ions, sugars, and amino acids) into the periplasm. Porins are important determinants of the pathogenicity and virulence of infections by pathogenic *E. coli*. (Nikaido 1992; Schirmer 1998; Buchanan 1999; Schulz 2000; Achouak et al. 2001; Delcour 2003; Benz 2004).

Porins were the first membrane proteins crystallized for X-ray diffraction (Garavito and Rosenbusch 1980). The

J. Giri · J. M. Tang · B. Eisenberg (✉)
Department of Molecular Biophysics and Physiology, Rush University, 1750 W. Harrison St., Chicago, IL 60612, USA
e-mail: beisenbe@rush.edu

J. Giri
Department of Bioengineering, University of Illinois at Chicago, Chicago, IL 60607, USA

C. Wirth · C. M. Peneff
Department of Structural Biology, Biozentrum, University of Basel, Klingelbergstrasse 70, 4056 Basel, Switzerland

Published online: 13 January 2012

structures of many porins are now known, including the classic porins OmpF, PhoE (Cowan et al. 1992), and OmpC (Baslé et al. 2006), and the specific porins LamB (Schirmer et al. 1995) and TolC (Koronakis et al. 2000). Indeed, more porin structures are known than of any other class of membrane passive transporters. The intrinsically strong structure of their β-barrels enables the porins to resist chemical and mechanical stress and, we believe, make the protein easier to crystallize. (However, not all porins crystallize easily, for unknown reasons.)

The molecular mechanisms underlying the diverse roles and survival of porins can be studied by use of structural and functional measurements, and by molecular modeling. Purified porins are readily available in large amounts. Their biophysical and biological functions have been characterized by use of state of the art electrophysiological techniques, for example patch-clamp and planar lipid bilayer reconstitution (Delcour 1997). The detailed characterization of porins reveals the fundamental mechanisms that determine the functional properties of physiological ion channels with molecular or even atomic resolution. Detailed characterization helps in the design and construction (i.e., "engineering") of porins with desired functions (Miedema et al. 2004; Vrouenraets et al. 2006; Bayley 2005; Miedema et al. 2007).

Porins are usually classified as either general non-specific porins or solute-specific porins. The general porins OmpF, OmpC, and PhoE of *E. coli* are channels that allow passive diffusion of small solutes (under 600 Da) down their electrochemical gradient. The general porins transport a variety of substances and do not have a marked preference for particular solutes. "Specific" porins have preference for particular solutes, for example, the maltoporin LamB (Benz et al. 1987) of *E. coli* selectively transports maltose. The genes of these specific solute-transporting porins are generally induced by special growth conditions that also induce the protein machinery needed to metabolize the acquired solute transported by the specific porins. The specific porins are needed for the bacteria to thrive under the special inducing conditions and are usually not expressed (in substantial quantities) unless those conditions are present.

NanC belongs to this class of porins and its expression is induced by the presence of *N*-acetylneuraminic acid (Neu5Ac), the most abundant of the sialic acids. Sialic acids are nine-carbon negatively charged sugar molecules that, together, compose a family of more than 40 members (Comb and Roseman 1960). The sugars are found primarily at the terminal positions of many glycoconjugates present in the outer leaflet of the cell membranes of eukaryotes. Pathogenic bacteria often use the sialic acids of the host as sources of carbon, nitrogen, and amino sugars taking advantage of their exposure to the extracellular space. The ability of the bacteria to colonize, persist, and cause disease (Vimr et al. 2004; Severi et al. 2007) depends on their ability to use sialic acids, in many cases. Thus, the properties of NanC are of clinical interest to microbiologists.

Most animal tissues contain free sialic acid (Vimr et al. 2004) that can flow through NanC and serve as the main carbon source for *E. coli*. OmpF/OmpC are often not expressed by *E. coli* (Condemine et al. 2005) (for reasons unknown to us). When OmpF/OmpC are not expressed by the *E. coli* bacteria, NanC must be present (i.e., it must be induced) to promote efficient uptake of Neu5Ac across the outer membrane. In those cases the properties of NanC directly control the life of the bacteria: induction is not an artificially contrived situation that only occurs in the laboratory.

The functional role of induction of the sialic acid-specific uptake systems has been demonstrated in many ways under many conditions. The classical approaches include growth experiments and liposome-swelling experiments (Nikaido 1992; Nikaido 2003). In growth experiments, the role of a specific membrane protein (or a transport system) is demonstrated by monitoring the growth of the wild type bacteria and comparing it with that of "knock out" mutant bacterial strains that are missing specific proteins. Growth is studied under controlled conditions in external solutions ("growth media") enriched in or deprived of a particular solute, for example, the maltodextrin-specific transport system in *E. coli* (Wandersman and Schwartz 1982). In liposome-swelling experiments, the specificity of a membrane protein for a particular solute is demonstrated by monitoring the rate of swelling of protein-containing liposomes under different solutions. For example, swelling can be measured in liposomes containing the LamB protein of *E. coli* (Benz et al. 1987). These classic techniques are responsible for most of our knowledge of transport in bacteria and enable biophysical analysis of specific uptake systems. Biophysical analysis is needed to reveal the mechanistic details of the uptake system at molecular and atomic resolution. For example, membrane proteins must be characterized using the patch-clamp or the planar lipid bilayer methods of channel biology to unravel the underlying mechanisms of transport through single protein molecules (Miller 1986; Sakmann and Neher 1995).

We characterize the functional properties of NanC by use of electrophysiological methods, because these enable measurements of the current flow through single channels with a 0.1-ms time scale. Classical assays of NanC function measure the properties of macroscopic numbers of channels embedded at unknown density in the outer membrane of bacteria and have time resolution of seconds or even minutes.

Recently, a high resolution structure of NanC has been reported (Wirth et al. 2009). The structure of NanC has

many of the features of other outer membrane channel proteins. NanC is a monomer, a 12-stranded β-barrel with a relatively narrow pore of average diameter 6.6 Å. However, NanC is also different in many ways from other porin structures. In most of the porins, a "loop" of a polypeptide chain partially occludes the pore region and is the most obvious location where specific interactions and gating might occur. Interestingly, NanC has no "loop" occluding the pore. The pore region of NanC is predominately decorated by positively charged residues that are arranged to form two positively charged tracks facing each other across the pore. This particular arrangement of the positively charged residues in the pore region seems to help the negatively charged Neu5Ac to move through NanC. The carboxylate group (COO^-) of Neu5Ac is charged ("deprotonated") at physiological pH, because its $pK_a \approx 2.6$. The positively charged tracks are likely to guide the movement of negatively charged solutes the way the steel tracks of a railroad guide trains, both passive passenger cars and active locomotives. The fixed charges create an environment similar to that of the ion exchangers studied by physical chemists and biophysicists decades ago (Teorell 1953; Helfferich 1962; Karreman and Eisenman 1962; Conti and Eisenman 1965; Walker and Eisenman 1966; Eisenman et al. 1967; Eisenman and Horn 1983).

Earlier patch-clamp measurements of NanC did not reveal a significant change in the function of NanC in the presence of even large concentrations of Neu5Ac, up to 50 mM (Condemine et al. 2005), perhaps because the ionic conditions and buffer used masked the effect of the sialic acid. The high-resolution structure has many basic (positive) side chains that would be screened (Chazalviel 1999) in the high salt concentrations used in these earlier measurements. Structural measurements also show HEPES binding to NanC. Two HEPES molecules were immobile enough under crystallizing conditions to cause diffraction in the crystal structure, one near each end of the channel. Binding strong enough to crystallize HEPES in place in a crystallized channel seems likely to modify current flow through the native channel, despite the different ionic conditions.

Our objective is to characterize the biophysical properties of NanC and determine the baseline experimental conditions necessary for measurement of the transport of Neu5Ac in bilayers. We seek biophysical conditions that result in biological transport. We determine the ionic conditions suitable for single-channel measurements of NanC in an artificial lipid bilayer and then measure the ion selectivity and conductance of the channel. Many years of experience with single-channel recording (Miller 1986; Sakmann and Neher 1995) reveal the need for care and calibration if results of biological importance are to be reproducible in many laboratories. Single-channel measurements are prone to electrical artifact and cannot be performed reliably without specialized hands-on training in electrophysiology. In our case, detailed analysis was necessary to show that buffers used widely, if not universally, in biochemical experiments interfere with the function of NanC. Buffers can block the channel. A suitable baseline solution for NanC is 250 mM KCl adjusted to pH 7.0 without buffer. An unexpected artifact was a significant impediment to our work and is emphasized here because private discussions show this to be a widespread (but not understood) problem: TRIS in the baths reacts with Ag/AgCl electrodes, producing artifacts even when the electrodes are on the far side of agar–KCl bridges.

Materials and methods

NanC expression and purification

NanC was expressed in BL21/Omp8 strains and purified as reported elsewhere (Wirth et al. 2009). After cell disruption, the whole membranes were pelleted by ultracentrifugation (1 h at 100,000 g). The inner membrane was solubilized by use of 1% lauroyl sarcosine and the remaining outer-membrane was collected by ultracentrifugation. NanC protein was solubilized from the membrane by iterative extractions with increasing concentrations of octylpolyoxyethylene (OPOE). NanC was then purified by anion-exchange chromatography followed by cation-exchange chromatography. Final size-exclusion chromatography (Superdex75, GE Healthcare) enabled exchange of the buffer to 10 mM Tris pH 8.0, 150 mM NaCl, and 1% OPOE in which the protein was stored.

Electrophysiology

Chemicals and solutions

Chemicals were purchased from Sigma-Aldrich and Fisher Scientific. The lipid cocktail solution (DOPE:DOPC) used for bilayer experiments was from Avanti Polar Lipids. The salt solutions used (with or without pH buffers) were adjusted to pH 7.4 or 7.0. The pH of the salt solution was monitored carefully by checking the pH at the beginning and end of the experiment. For salt solutions (without buffer) no significant drift in pH was noticed.

Planar lipid bilayer experiments

Electrophysiological measurements of current flow through the channel proteins can be performed by either the patch-clamp or planar lipid bilayer method (Boulton et al. 1995; Molleman 2003; Miller 1986; Sattelle 1993; Tien and

Ottova-Lietmannova 2003). In the planar lipid bilayer method (Mueller et al. 1962) electrical measurements of the channel proteins are carried out in an artificial lipid membrane with proteins inserted into the bilayer. In the patch-clamp method (Neher and Sakmann 1976; Hamill et al. 1981), measurements are conducted in native cell membranes. Both methods are widely used for single-channel measurements (Colquhoun and Sigworth 1983; Sakmann and Neher 1995).

We use the planar lipid bilayer method to measure the functional properties of purified channel protein NanC. We insert a single molecule of NanC into a preformed lipid bilayer by use of the set-up shown in Fig. 1, which also shows the main components of the bilayer. The bilayer set-up consists of a chamber and a Delrin cup that are filled with aqueous solutions. A magnetic stirrer driven by batteries is used for stirring the solutions.

We use the painted technique to form the planar lipid bilayer. In this method the lipid bilayer is formed by painting a lipid solution across a 150 μm diameter aperture in the cup. The stability of the lipid bilayer is increased if the aperture is pretreated ("primed") with the lipid solution before the bilayer is formed.

The lipid solution is made of phospholipids DOPE:-DOPC in 4:1 ratio (*v*/*v*) dissolved in *n*-decane as solvent (10 mg/ml). The solvent orients the monolayers of lipids to form a bilayer. Initially, a thick film of lipid solution is formed; this eventually thins as the solvent evaporates and a lipid bilayer is obtained. A "healthy" (presumably thin) lipid bilayer is essential to ensure incorporation of the protein. Membrane thickness is measured by determination

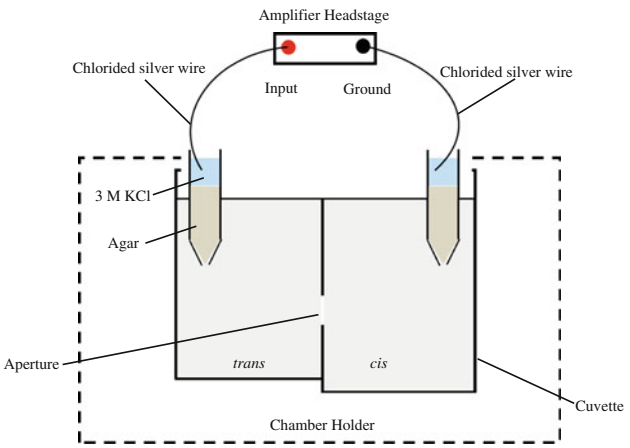

Fig. 1 Bilayer setup for single-channel measurements: The *cis* (ground) and *trans* (voltage) compartments are filled with aqueous salt solutions. The chlorided silver (Ag/AgCl) wires are the electrodes connecting the baths via agar–KCl salt bridges. An artificial lipid bilayer is painted over the aperture. The voltage applied across the lipid membrane is $V_m = V_{trans} - V_{cis}$. Protein solution (~0.1–0.2 μl) is added to the *cis* compartment and stirred to initiate incorporation of a single channel into the bilayer

of membrane capacitance. In our set-up, the electrical capacitance of a "healthy" lipid bilayer is 60–80 pF with a specific capacity of ~0.4 to 0.6 μF per cm^2.

Membrane proteins are inserted into the bilayer in different ways depending on their water solubility. We used direct fusion to insert a single molecule of NanC into the lipid bilayer. Note that membrane proteins are often not water soluble and, therefore, detergent is added to its stock solution to make a soluble mixture of protein and detergent. The effect of the detergent on protein function must be checked, in every case. We use a stock solution of ~1.1 μg/ml of the purified NanC in 150 mM NaCl, 10 mM Tris, pH 8.0 containing 1% (*v*/*v*) n-OPOE detergent. We add ~0.1 to 0.2 μl of the stock solution to the *cis* or *ground* side of a stirred solution to insert NanC. The ground side is the side of the bilayer connected through a bath electrode to zero (ground or earth potential).

In our set-up Ag/AgCl electrodes are used to connect the solutions in the *cis* compartment to ground and the *trans* compartment (the voltage side of the bilayer) to the patch clamp amplifier. Ag/AgCl electrodes are stable, robust, and the most commonly used electrodes in electrophysiology but they respond to the activity of Cl^-. They respond to Cl^- concentration and electrical potential, approximately as described by the classical Nernst equation of electrochemistry (Bard and Faulkner 2000). The Ag/AgCl electrodes are isolated from bathing solutions by agar bridges (2%) containing (typically) 3 M KCl. The 3 M KCl provides a fixed stable Cl^- concentration for the Ag/AgCl wire so the electrode potential is stable and minimal. Changes in the electrical potential in the wire are produced by changes in the electrical potential in the surrounding solution, not by changes in the activity of Cl^-, because the chloride concentration is constant near the electrode in this setup. A so-called liquid junction potential (LJP) appears, of course, at the interface of the 3 M KCl agar with the bath solutions. This potential is small because the mobility of K^+ and Cl^- are nearly equal. We determined the LJP from the junction potential calculator (JPCalcW) made available by Molecular Devices with their PClamp package (Barry 1994, 1996–2009) based on publications by Barry and Diamond (1970), Barry (1989), and Barry (1994). The range of LJP under the ionic conditions we used for the reversal potential measurements was between −0.7 mV and −1.2 mV (Table 1). The LJP calculator JPCalcW is based on the reduced models of liquid junction potentials that uses the generalized Henderson liquid junction potential equation (Bard and Faulkner 2000; Barry and Diamond 1970; Barry 1989; Barry and Lynch 1991; Morf 1981; Amman 1986). This equation is not customarily derived by mathematics from the appropriate description of nonideal solutions (necessary when salt concentrations are high as they are in and near the salt bridge). We look forward to such

Table 1 Measurement of the ion selectivity of a single NanC molecule in the bilayer. Reversal potential V_{rev} measured in the presence of an ionic gradient in the *cis* (250 mM KCl, pH 7.0) and *trans* (1 M/3 M KCl, pH 7.0) compartments compared with the calculated Nernst potentials E_K^+ and E_{Cl}^- under those conditions

Experiment	*cis* (ground) KCl (mM)	*trans* (voltage) KCl (mM)	LJP (mV)	E_{Cl}^- (mV)	E_K^+ (mV)	V_{rev}^* (mV)
1	250	1,000	−0.7	+35	−35	+15.89 ± 1.01 ($N = 2$)
2	250	3,000	−1.2	+63	−63	+ 28.31 ± 0.37 ($N = 9$)

The measured V_{rev} indicates the anion selectivity of NanC. V_{rev}^* is the reversal potential obtained after correction for the liquid junction potentials, with the standard error of the mean. N denotes the number of measurements

derivations in the future. The agar bridge has the further advantage that it keeps Ag^+ ions away from the bilayer and reconstituted channel. Ag^+ ions, even at very low concentrations, can be toxic (i.e., cause irreversible changes) to channels.

Pulse procedure and data analysis

Conductance is determined from measurements of current through a fully open single channel. The recording voltage pulse procedures used throughout the paper for the single-channel measurements of NanC in lipid bilayer are shown in Fig. 2. There are two main kinds: the step pulse procedure (A and B) and the ramp procedure (C and D). In step pulse procedures, the recordings are made at a fixed potential i.e., ±100 mV, ±150 mV etc. for a definite time period for example, 3 or 10 s. The amplitude of the single-channel current and the probabilities that the channel is open or closed are measured as the voltage is stepped from one value to another. However, the voltage across the channel follows a ramp time course. In the ramp pulse procedure the recordings are made for a range of potentials at which the channel is expected to be mostly open, for example, from +100 to −100 mV. We thus capture current through a single fully open channel. The duration of the voltage ramp is ∼2 s.

The data being recorded are low-pass-filtered at 2 kHz by use of the built-in analog low-pass Bessel filter in the Axopatch 200B amplifier (Molecular Devices) and is sampled or digitized at the 5 kHz rate that the Nyquist sampling theorem (and properties of the analog Bessel filter) implies is needed to avoid aliasing. After the recording, the recorded data are filtered digitally (at 300/500 Hz) for further analysis using the low-pass 8-pole digital Bessel filter in the PClamp software, version 10 (Molecular Devices).

Leakage subtraction and offset current correction

Two main corrections are performed on the recorded single-channel current–voltage traces after the digital filtering: leakage subtraction and offset current correction.

Leakage subtraction

Before addition of the protein sample, the *control* or the *baseline* current (Fig. 3b) is measured in response to the same voltage (ramp and step) pulse procedure under the same ionic conditions as in the experimental recordings.

Leakage is defined as the current that flows ("leaks") through the lipid bilayer without going through a channel and is measured as the conductance of the *control* or the *baseline* current trace. The leakage conductance is determined by estimating the slope of the *baseline* current trace recorded for the same voltage waveform that is applied while measuring the corresponding single-channel current recordings, for example, a definite voltage for the step pulse procedure or over a range of voltages for the ramp procedure.

The single-channel current–voltage recordings are (accordingly) corrected for leakage by subtracting the corresponding measured leakage conductance from the filtered single-channel current traces. This procedure is necessary in case the leakage conductance has nonlinear, ion-dependent, and/or time-dependent behavior, as is often the case.

Offset current correction

Under symmetric ionic conditions, i.e., when equal concentrations of ions are present on both sides of the bilayer, the current flowing through the single channel in a bilayer should be equal to zero at 0 mV, because the system is passive. However, under experimental situations various asymmetries in the apparatus usually drive a finite current even when the baths are identical. Current offset is this "residual" current that flows through the single channel in a bilayer at 0 mV under symmetric ionic conditions, i.e., with the same solution on both sides of the channel. Under symmetric ionic conditions, the single-channel current–voltage recordings are corrected for current offset (that arises from external artifactual sources) by subtracting the corresponding measured residual current from the filtered single-channel current traces.

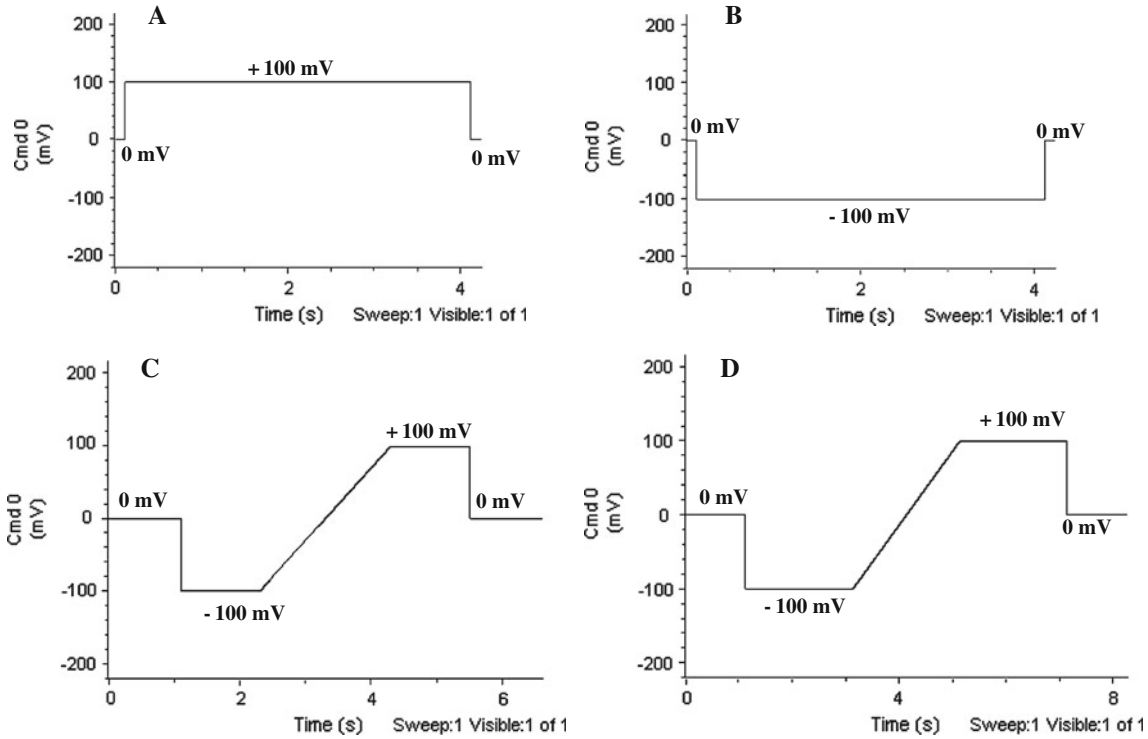

Fig. 2 Recording pulse procedures used throughout single-channel NanC conductance and selectivity measurements. **a** Positive step procedure in which the voltage is stepped up from 0 mV to +100 mV after ~1 s and stepped back to 0 mV after 4 s. Similar procedures are designed for voltages +150 mV and +200 mV. **b** Negative step procedure in which voltage is stepped down from 0 mV to −100 mV after ~1 s and set back to 0 mV after 4 s. Similar procedures are designed for voltages −150 mV and −200 mV. **c**. Ramp procedure in which voltage is stepped down from 0 mV to −100 mV after ~1 s. Voltage stays at −100 mV for 1 s and is then ramped to +100 mV for ~2 s staying at +100 mV for 1 s before being set back to 0 mV. **d** Ramp procedure in which voltage is stepped down from 0 mV to −100 mV after ~1 s. Voltage stays at −100 mV for 2 s and is then ramped to +100 mV for ~2 s staying at +100 mV for 2 s before being set back to 0 mV

However, under asymmetric ionic conditions—i.e., when unequal amounts of ions are present on both sides of the bilayer—the offset current is determined from the *control* or the *baseline* current that is measured before the channel protein is incorporated. The offset current under asymmetric ionic conditions contains the artifactual offset current already described. It also contains a diffusive current that flows through the leakage conductance, because of the ionic gradient across the lipid bilayer and leakage conductance. The single-channel current–voltage recordings under asymmetric ionic conditions are, accordingly, corrected for current offset by subtracting the corresponding measured diffusive current from the filtered single-channel current traces.

Terminology

The potential difference (V) is defined as, $V = V_{trans} - V_{cis}$ where *cis* represents the *ground* side of the chamber and *trans* is where we apply the *voltage*. A positive (outward) current (I) is defined as a flux of positive charge from *trans* to *cis*.

The measurement of reversal potential V_{rev} determines the ion selectivity of the channel in a predefined ionic gradient. The measured V_{rev} is corrected for measured liquid junction potentials (LJP, mentioned in the figure legends where applicable). The LJP is determined from the junction potential calculator (JPCalcW) made available by Molecular Devices with their PClamp package (Barry 1994, 1996–2009) and based on the Barry and Diamond (1970), Barry (1989), and Barry (1994). This admirable software is itself based on the classical Henderson equations which are not consistent with the Poisson equation of electrostatics, as they should be, as we have mentioned previously. Fortunately, the corrections are small (−0.7 to −1.2 mV; Table 1) so errors in the correction itself are insignificant in this work.

Conductance is defined as the slope conductance of the fully open single channel in the presence of equal concentrations of ions on both sides of the bilayer measured over a 60 mV interval ranging from −30 to +30 mV.

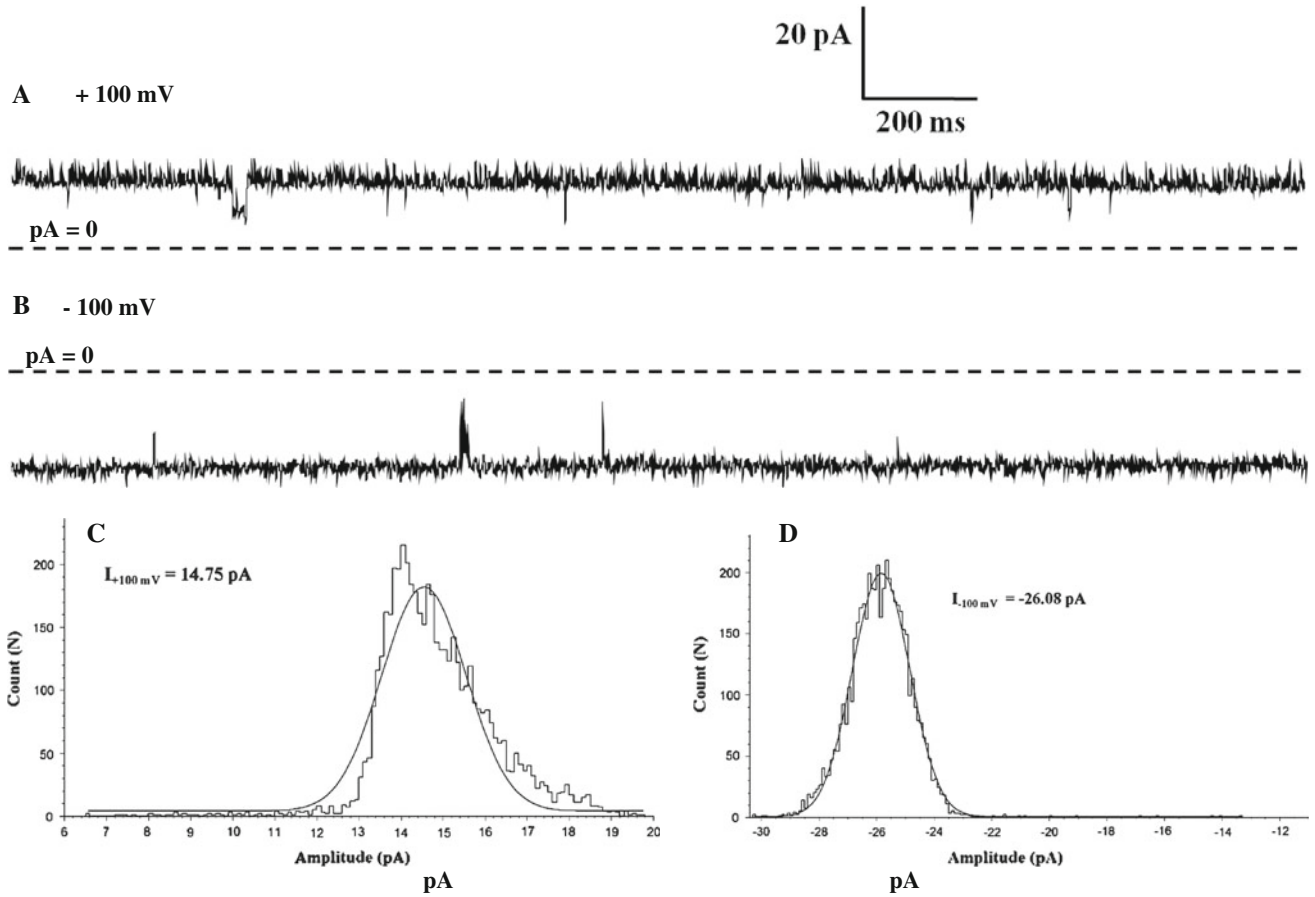

Fig. 3 Single-channel current of NanC in bilayer in the presence of symmetric 500 mM KCl, 20 mM HEPES, pH 7.4 shown at step voltages of +100 mV in **a** and −100 mV in **b**. *Dashed lines* represent zero current. The corresponding single-channel amplitudes are 14.75 pA at +100 mV and −26.08 pA at −100 mV, determined from amplitude histogram analysis as shown in **c** and **d**, respectively. In the bilayer at ±100 mV step voltages the single channel NanC is mostly open and asymmetric (non-equal) conductances are observed

Results

We have investigated the function of a single channel protein NanC in an artificial lipid bilayer using the planar lipid bilayer technique in order to identify appropriate ionic conditions that will enable study of the biological role of NanC in the transport of Neu5Ac across the outer-membrane of *E. coli* (Condemine et al. 2005; Wirth et al. 2009).

We first designed experiments that would reproduce the single-channel measurements of NanC reported by Condemine et al. (2005). In these experiments we measured single-channel current and unit slope conductance in the presence of symmetric, i.e., equal ion concentrations on both sides of the bilayer, 500 mM KCl, 20 mM HEPES, pH 7.4 at different applied step voltages ±100 and ±200 mV and ramp voltage as shown in Figs. 3, 4, and 5 respectively.

NanC has voltage-dependent gating (Figs. 3 and 4). NanC is mostly open at voltages ≤100 mV and closed at voltages ≥200 mV in bilayer. Single-channel current amplitudes shown were determined from analysis of amplitude histograms.

NanC has a large unit (slope) conductance. We measured the unit slope conductance by following the sequence of steps shown in Fig. 5. First, the "baseline" current (as shown in Fig. 5b) was measured. We measured the current in response to the voltage ramp pulse procedure shown in Fig. 5a *before* a channel was inserted into the lipid bilayer. The current measured through the reconstituted single channel NanC in the bilayer is shown in Fig. 5c. The offset and the leakage current correction were carried out as described in the "Materials and methods" section and the resulting single-channel current–voltage trace is shown in Fig. 5d. The unit conductance was determined from the slope measured in the voltage-range between the dashed lines.

During these experiments we found that NanC operated in two-modes. In the first mode, a single channel of NanC had two states, i.e., one open state and one closed state. In the second mode, NanC had two distinct open states, that we called sub-conductance states, and one closed state. In Fig. 6 we have shown the two distinct sub-conductance levels. The corresponding amplitudes at ±100 mV were

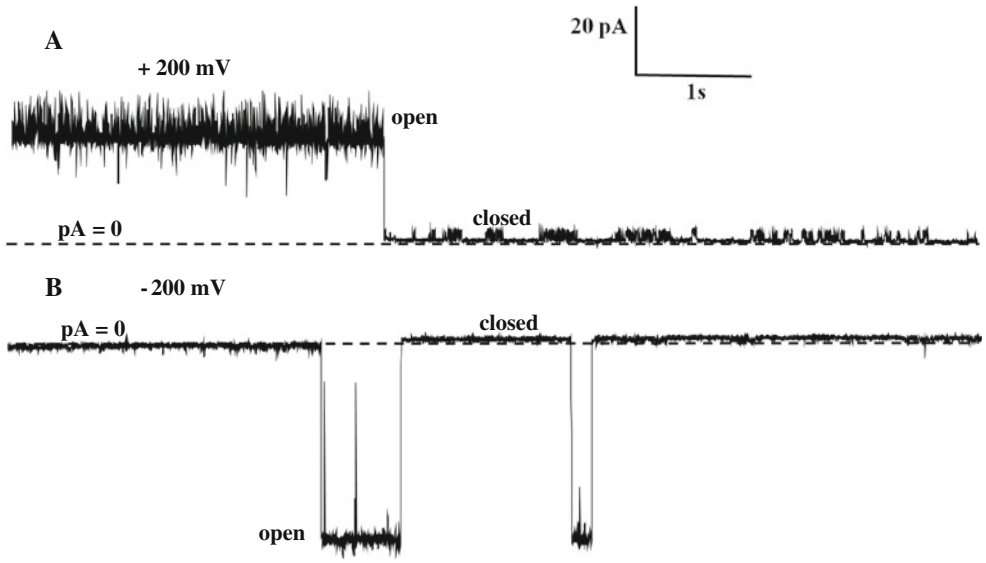

Fig. 4 Single-channel current of NanC in the bilayer in the presence of symmetric 500 mM KCl, 20 mM HEPES, pH 7.4 shown at step voltages of +200 mV in **a** and −200 mV in **b**. *Dashed lines* represent zero current. The corresponding single-channel amplitudes are 27.71 pA at +200 mV and −53.78 pA at −200 mV, determined from amplitude *histogram* analysis as shown in c and d, respectively, of Fig. 3. In the bilayer step voltages of ±200 mV cause closure of NanC

determined from the amplitude histograms. The distinct sub-conductance levels were not observed in the first mode (Fig. 3). These sub-conductance states were not induced by the ionic conditions present. They were found in the presence of buffer—for example, HEPES/Phosphate—or without buffer and they were found at high salt concentration. Note that the second mode of NanC occurred in only a small fraction of experiments. We report it nonetheless because it was observed many times. These observations indicate that native Nanc has both modes of operation.

The next step was to search for ionic conditions that would enable us to study Neu5Ac transport through NanC. While looking for these experimental conditions, we found that HEPES buffer interfered with the function of NanC and reduced the ionic current carried by NanC as shown Fig. 7. This result was expected because the NanC structure reported in the Protein Data Bank (PDB code: 2WJR) contains two HEPES molecules bound to the channel. HEPES reduced the single channel conductance of NanC substantially. Similar blocking action of HEPES had been observed in other anion channels also (Yamamoto and Suzuki 1987; Hanrahan and Tabcharani 1990). In biological cells HEPES is not found and so its effects should not be the focus of physiological attention. However, the native functional properties of NanC should be investigated experimentally without HEPES.

We investigated use of alternative pH buffers instead of HEPES, because we did not wish to study a blocked channel. We found that the (classic inorganic) phosphate buffer (a buffer commonly used in electrophysiology experiments on anion channels) interfered with the channel's ionic conductance. The unitary ionic conductance of NanC decreased substantially in the presence of the negatively charged phosphate. There was a 19% drop in unitary ionic conductance of NanC when phosphate concentration was increased from 0 mM (114.096 ± 4.16 pS, $N = 12$, control) to 5 mM (92.07 ± 0.657 pS, $N = 11$) in 250 mM KCl, pH 8.0, where N is the number of measurements.

The effect of phosphate buffer on the ionic current carried by a unit NanC in bilayer seemed to be less dramatic than that of HEPES. In comparison with the control experiment (250 mM KCl, pH 7.0 without buffer) the presence of 5 mM HEPES in 250 mM KCl at pH 7.4 (70.70 ± 5.17 pS, $N = 15$) resulted in a 38% drop in unit ionic conductance of NanC whereas the same amount of phosphate resulted in a 19% drop. We thus report that these commonly used pH buffers (HEPES and phosphate) substantially affect the functional behavior of a unit NanC in a bilayer. Therefore these pH buffers (HEPES and phosphate) are not recommended for use in salt solutions while studying the native functional properties of NanC at the single-channel level.

TRIS (another commonly used buffer) damaged the Ag/AgCl electrodes in our set-up, even though the electrodes were separated from the buffer by an agar/KCl bridge. The action of TRIS on the Ag/AgCl electrodes even in presence of agar/KCl bridges was puzzling and did not result in any interpretable measurements.

We therefore decided to study NanC (conductance vs. concentration and ionic selectivity) in ionic solutions that were adjusted to pH 7.0 but without using a pH buffer.

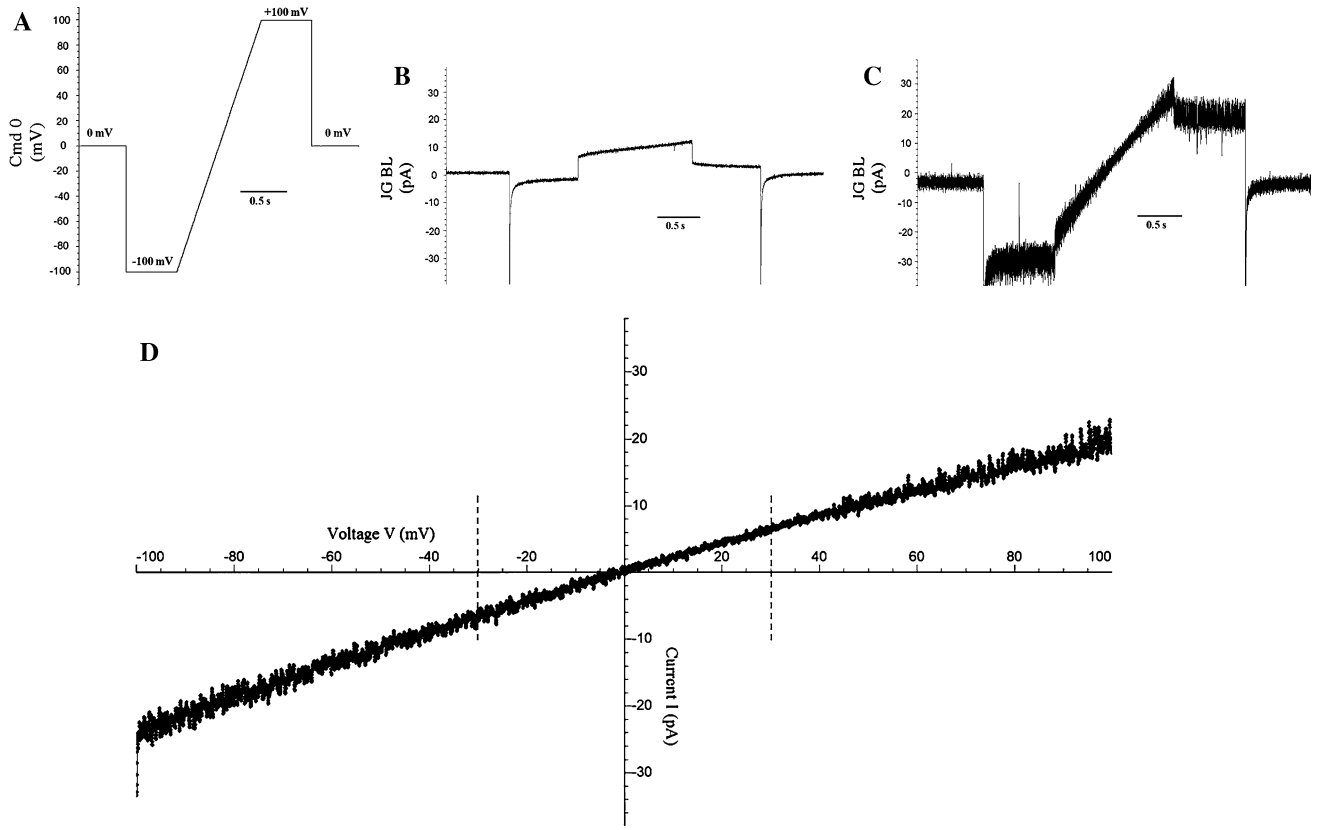

Fig. 5 Measurement of single-channel slope conductance of NanC in the lipid bilayer. **a** Ramp voltage pulse procedure. Voltage is stepped down from 0 mV to −100 mV after ∼1 s. Voltage stays at −100 mV for 1 s and is then ramped to +100 mV for ∼2 s staying at +100 mV for 1 s before being set back to 0 mV. **b**. Baseline current recorded in response to the ramp voltage pulse procedure as shown in **a**, through the lipid bilayer before the channel reconstitutes in symmetric (i.e. same ionic conditions in *cis* and *trans*) 500 mM KCl, 20 mM HEPES, pH 7.4. The baseline current trace filtered digitally at 300 Hz is shown. **c**. Single-channel current recorded as NanC reconstitutes in the lipid bilayer. The single-channel current trace filtered digitally at 300 Hz is shown. **d**. Single-channel current (I)−voltage (V) trace shown after correction for leakage and offset currents by following the procedures mentioned in the "Materials and methods" section. *Dashed lines* represent the −30 mV to +30 mV range chosen for determining the slope conductance given as $g(\mathrm{nS}) = \frac{\Delta \mathrm{I(pA)}}{\Delta\ \mathrm{V\ (mV)}}$, where g is the single channel conductance obtained as the slope of the I–V trace over the 60 mV range. The measured single-channel slope conductance of NanC in symmetric 500 mM KCl, 20 mM HEPES, pH 7.4 is 215.80 ± 0.96 pS, ($n = 15$)

This was the only way we could study a channel that was not blocked, assuming of course that the $\sim 10^{-7}$ M hydroxyl ion present in water at pH 7.0 did not itself block the channel.

We first measured the single-channel current–voltage behavior of NanC in solutions containing KCl at a range of concentrations (100 mM–3 M) without any buffer, as shown in Fig. 8. We observed that the single-channel current carried by NanC increased with increasing KCl concentration. We chose 250 mM for further experiments, because at larger salt concentrations (≥500 mM) screening is large enough to change the net charge of the "pore" region and the function of NanC.

We further measured the reversal potential shown in Fig. 9 to determine the ion selectivity of a single molecule of NanC in the bilayer. We expected selectivity for anions because the crystal structure of NanC revealed two tracks of positively charged residues in the pore region. The Nernst potential gives a measure of the gradient of the chemical potential. If NanC were a cation channel, then $V_{rev} = E_K$. If NanC were an anion channel, then $V_{rev} = E_{Cl^-}$. The negative direction of current at 0 mV and the measured value of the V_{rev} (close to E_{Cl^-}) indicated that NanC was an anion channel. It was more permeable for the anion Cl^- than the cation K^+. The reversal potentials for a single molecule of NanC in the bilayer under different ionic gradients are listed in Table 1.

Discussion

Single-channel bilayer experiments with NanC are feasible using standard methods implemented carefully and can be conducted with high "yield" in many conditions. The

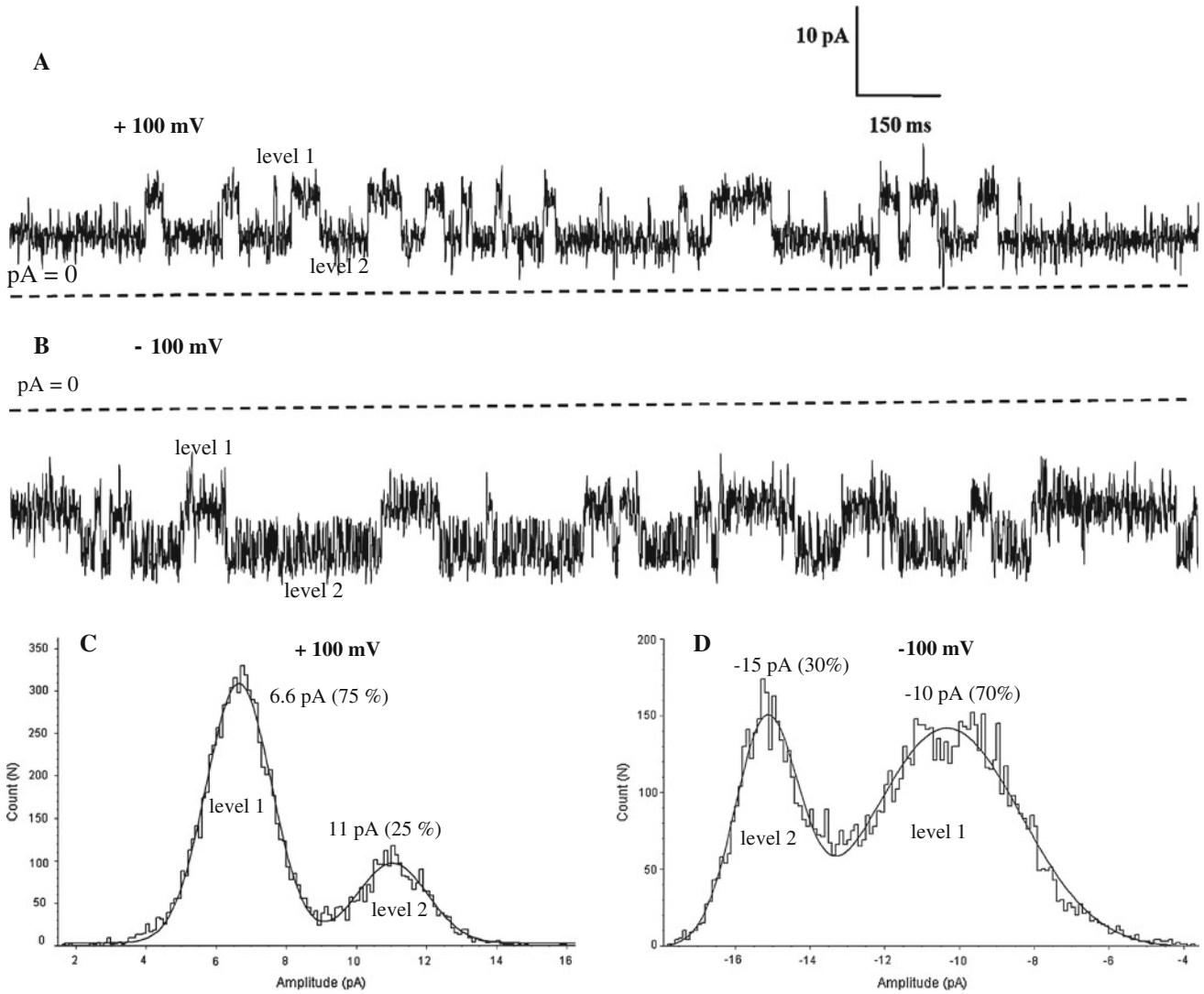

Fig. 6 The two distinct sub-conductance states of single channel NanC in the bilayer shown in symmetric 250 mM KCl, pH 7.0 at + and −100 mV voltages in **a** and **b** respectively. The amplitudes of the two current levels shown in **c** and **d** are determined by amplitude histogram analysis of the traces as shown in **a** and **b**. Percentage values in parentheses denote the probability the channel stays in the corresponding level for the duration the measurement. Sub-conductance states are native to the NanC and not induced by the experimental conditions, i.e. in the presence of buffer, for example, HEPES/phosphate, or without buffer and high salt concentration. The sub-conductance states did not occur so often ($\sim$<5%). The current traces shown are filtered digitally at 500 Hz. *Dashed lines* represent zero current

experiments show the biophysical properties of ion selectivity, conductance, and gating. NanC functions as a monomer, and has large conductance, anion selectivity, and two distinct modes of function (with or without sub-states).

The interactions of the commonly used pH buffers in electrophysiology experiments (HEPES, phosphate and TRIS) with NanC are interesting. HEPES binds to the pore region (as seen in the crystal structure) and actually reduces the ionic current carried by a single molecule of NanC in bilayer. Phosphate buffer reduces the unit ionic conductance of NanC. The negatively charged phosphate ions seem to compete with the chloride ions, resulting in a significant drop in unit ionic conductance. TRIS damages the electrodes even when salt bridges are present, making it impossible to record single-channel currents.

The measurements that we report here were thus carried out in ionic solutions adjusted to neutral pH without any buffer. We were careful to measure the pH of the ionic solutions before and at the end of the experiments to be sure that pH had not drifted. We found no drift and so we can carry out measurements of the biological function of NanC without buffer. We can measure Neu5Ac transport in salt

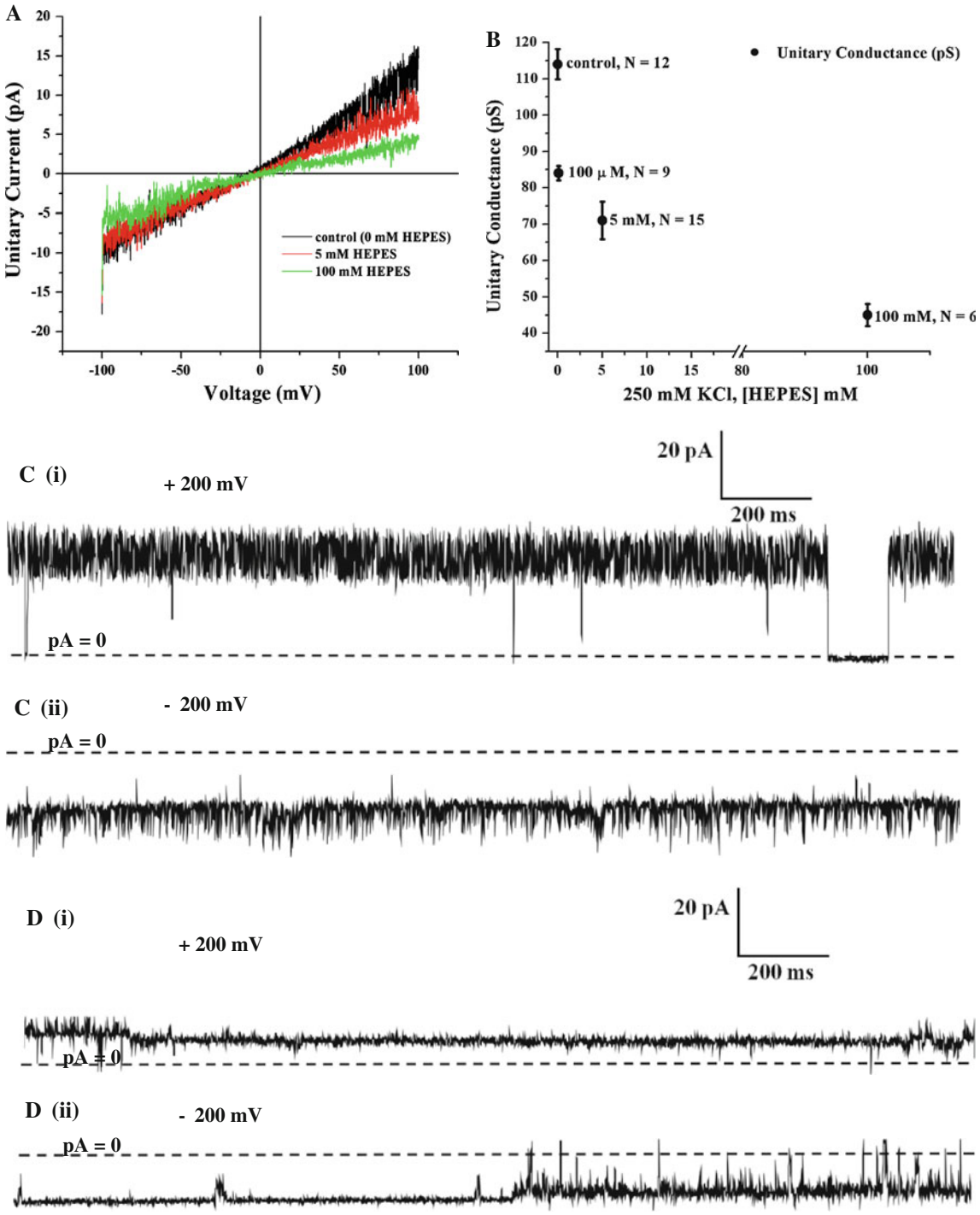

Fig. 7 Effect of the buffer HEPES on the single-channel current carried by NanC in the bilayer. **a**. Single-channel current (I)–voltage (V) traces measured in the presence of different concentrations of the buffer HEPES (0 mM (control in *black*), 5 mM (*red*) and 100 mM (*green*)) in 250 mM KCl on both sides of the bilayer. The current traces are filtered digitally at 300 Hz. The single-channel current decreases as the concentration of HEPES is increased with 250 mM KCl on both sides of the bilayer. HEPES binds to the channel's pore and reduces the unitary current as shown in **a**. The current traces are filtered digitally at 300 Hz. **b** Single-channel slope conductance measured as the concentration of HEPES is varied from 0 mM to 100 mM in 250 mM KCl on both sides of the bilayer. The unitary slope conductance decreases significantly as the concentration of HEPES increases. *N* is the number of measurements and the *error bars* represent the standard error of the mean. **c** (*i*) and (*ii*). Control single-channel current carried at +200 and −200 mV, respectively, in the presence of symmetric 250 mM KCl, pH 7.0 without HEPES. **d** (*i*) and (*ii*). Single-channel current carried at +200 and −200 mV, respectively, in the presence of symmetric 250 mM KCl, 100 mM HEPES, pH 7.0. The unitary current decreases by ∼50% compared with the control (0 mM) because of HEPES. Long closures are seen at ±200 mV. The current traces are digitally filtered at 500 Hz

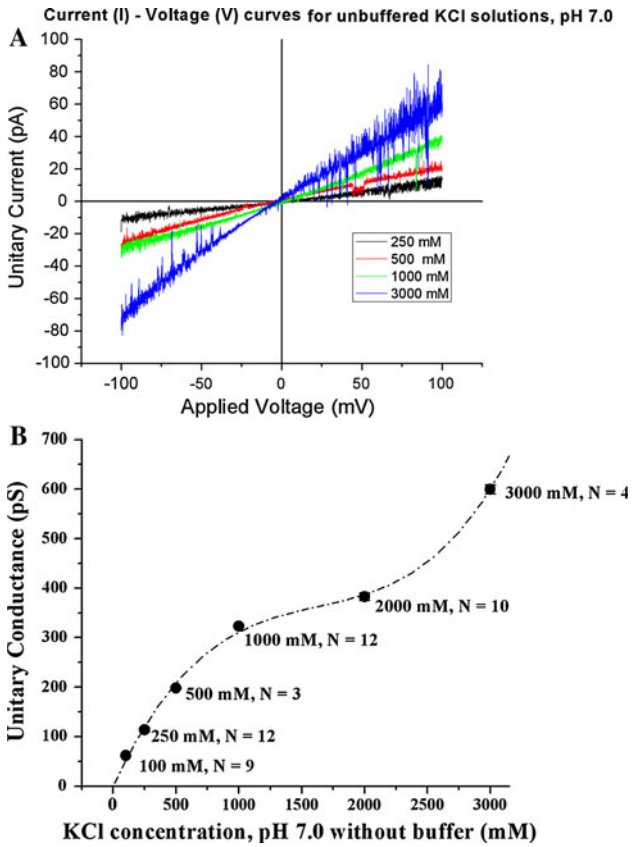

Fig. 8 **a** Single-channel current (I)−voltage (V)–concentration (*C*) traces measured in the presence of symmetric KCl, pH 7.0 (without buffer), shown as KCl concentration is varied from 250 mM to 3 M. The unitary current carried by NanC in the bilayer increases as the concentration of KCl is increased. The current traces shown in **a** are filtered digitally at 300 Hz. **b** Unit slope conductance of NanC determined in KCl salt solutions from 100 mM to 3 M, pH 7.0 (without buffer). *N* denotes the number of measurements and the *error bars* (too small to be seen) are the standard error of the mean. The unit slope conductance is determined over the 60 mV range as described in the "Materials and methods" section. The *dotted line curve* was obtained by polynomial fitting to the measured unit slope conductance data. The single-channel slope conductance of NanC increases as the KCl concentration is increased. From these measurements, we chose 250 mM KCl, pH 7.0 (without buffer) as the working solution for further experiments

solutions at concentrations of approximately 250 mM at pH 7.0.

Future work would benefit from the discovery of pH buffers that do not modify NanC's function in the lipid bilayer.

Acknowledgments We thank Tilman Schirmer for sharing with us his experience and insight on porins and proteins. We are grateful for continual discussions with Tilman, Dirk Gillespie, Dezső Boda, and Jim Fonseca. Dr Guy Condemine was most generous in providing materials and welcoming us to this field of research. Funding was provided by NIH grant GM076013.

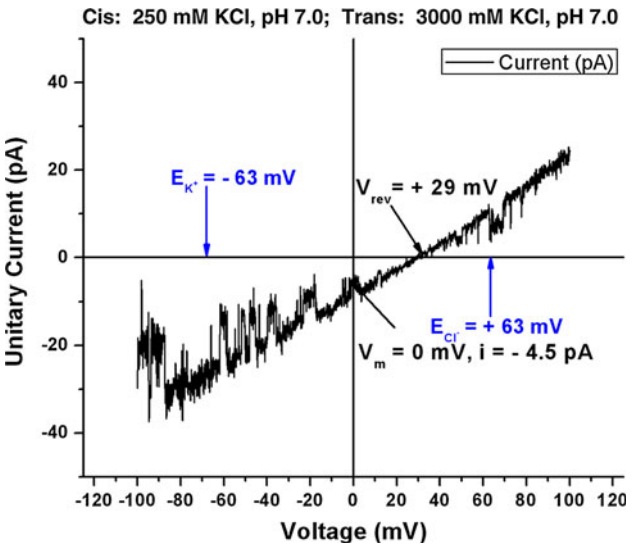

Fig. 9 Measurement of the reversal potential of a single molecule of NanC in the bilayer in the presence of 250 mM KCl (*cis*) and 3 M KCl (*trans*). The calculated Nernst potentials E_K and E_{Cl} are compared with the measured V_{rev}. At 0 mV, the current is negative and V^*_{rev} (corrected for liquid junction potential, LJP) is close to E_{Cl} because NanC is anion-selective. The current trace shown is filtered digitally at 300 Hz

References

Achouak W, Heulin T, Pagees JM (2001) Multiple facets of bacterial porins. FEMS Microbiol Lett 199:1–7

Amman D (1986) Ion-selective microelectrodes. Springer, Berlin

Bard AJ, Faulkner LR (2000) Electrochemical methods: fundamentals and applications, 2nd edn. Wiley, New York

Barry PH (1989) Permeation mechanisms in epithelia: biionic potentials, dilution potentials, conductances and streming potentials. In: methods in enzymology, biomembranes, part M: biological transport, vol 171, pp 678–715

Barry PH (1994) JPCalc, a software package for calculating liquid junction potential corrections in patch-clamp, intracellular, epithelial and bilayer measurements and for correcting junction potential measurements. J Neurosci Methods 51(1):107–116

Barry PH (1996–2009) JPCalc for windows (JPCalcW) Junction potential calculator users' manual. http://web.med.unsw.edu.au/phbsoft/JPCalcWManual-web-2009.pdf

Barry PH, Diamond JM (1970) Junction potential, electrode standard potentials, and other problems in interpreting electrical properties of membranes. J Membr Biol 3:93–122

Barry PH, Lynch JW (1991) Topical review: liquid junction potentials and small cell effects in patch clamp analysis. J Membr Biol 121:101–117

Baslé A, Rummel G, Storici P, Rosenbusch JP, Tilman S (2006) Crystal structure of osmoporin OmpC from *E. coli* at 2.0 A. J Mol Biol 362(5):933–942

Bayley H (2005) Engineered nanopores. In: Niemeyer CM, Mirkin CA (eds) Nanobiotechnology. Wiley, Weinheim

Benz R (ed) (2004) Bacterial and eukaryotic porins: structure, function, mechanism. Wiley, Vch

Benz R, Schmid A, Vos-Scheperkeuter GH (1987) Mechanism of sugar transport through the sugar-specific LamB channel of Escherichia coli outer membrane. J Membr Biol 100(1):21–29

Boulton AA, Baker GB, Walz W (1995) Patch clamp applications and protocols. Humana Press, Totowa

Buchanan SK (1999) Beta barrel proteins from bacterial outer membranes: structure, function and refolding. Curr Opin Struct Biol 9:455–461

Chazalviel J-N (1999) Coulomb screening by mobile charges. Birkhäuser, New York

Colquhoun D, Sigworth FJ (1983) Single-channel recording. Plenum Press, New York

Comb DG, Roseman S (1960) I. The structure and enzymatic synthesis of N-acetylneuraminic acid. J Biol Chem 235(9): 2529–2537

Condemine G, Berrier C, Plumbridge J, Ghazi A (2005) Function and expression of an N-acetylneuraminic acid-inducible outer membrane channel in Escherichia coli. J Bacteriol 187(6):1959–1965. doi:10.1128/JB.187.6.1959-1965.2005

Conti F, Eisenman G (1965) The steady state properties of ion exchange membranes with fixed sites. Biophys J 5(4):511–530

Cowan SW, Schirmer T, Rummel G, Steiert M, Ghosh R, Pauptit RA, Jansonius JN, Rosenbusch JP (1992) Crystal structures explain functional properties of two E. coli porins. Nature 358:727–733

Delcour AH (1997) Function and modulation of bacterial porins: insights from electrophysiology. FEMS Microbiol Lett 151(2): 115–123

Delcour AH (2003) Solute uptake through general porins. Front Biosci 8:1055–1071

Eisenman G, Horn R (1983) Ionic selectivity revisited: the role of kinetic and equilibrium processes in ion permeation through channels. J Membr Biol 76:197–225

Eisenman G, Sandblom JP, Walker JL Jr (1967) Membrane structure and ion permeation. Study of ion exchange membrane structure and function is relevant to analysis of biological ion permeation. Science 155(765):965–974

Garavito RM, Rosenbusch JP (1980) Three-dimensional crystals of an integral membrane protein: an initial X-ray analysis. J Cell Biol 86:327–329

Hamill OP, Marty A, Neher E, Sakmann B, Sigworth FJ (1981) Improved patch-clamp techniques for high-resolution current recording from cells and cell-free membrane patches. Pflugers Arch 391(2):85–100

Hanrahan JW, Tabcharani JA (1990) Inhibition of outwardly rectifying anion channel by HEPES and related buffers. J Membr Biol 116:65–77

Helfferich F (1962) Ion exchange. McGraw Hill, New York

Karreman G, Eisenman G (1962) Electrical potentials and ionic fluxes in ion exchangers. I. “n Type” non-ideal systems with zero current. Bull Math Biophys 24:413–427

Koronakis V, Scharrf A, Koronakis E, Luisi B, Hughes C (2000) Crystal structure of the bacterial membrane protein TolC central to mutlidrug efflux and protein export. Nature 405:914–919

Miedema H, Meter-Arkema A, Wierenga J, Tang J, Eisenberg B, Nonner W, Hektor H, Gillespie D, Meijberg W (2004) Permeation properties of an engineered bacterial OmpF porin containing the EEEE-locus of Ca2+ channels. Biophys J 87(5):3137–3147. doi:10.1529/biophysj.104.041384

Miedema H, Vrouenraets M, Wierenga J, Meijberg W, Robillard G, Eisenberg B (2007) A biological porin engineered into a molecular, nanofluidic diode. Nano Lett 7(9):2886–2891

Miller C (ed) (1986) Ion channel reconstitution. Plenum Press, New York

Molleman A (2003) Patch clamping: an introductory guide to patch clamp electrophysiology. Wiley, New York

Morf WE (1981) The principles of ion-selective electrodes and of membrane transport. Elsevier, Amsterdam

Mueller P, Rudin DO, Ti Tien H, Wescott WO (1962) Reconstitution of cell membrane structure in vitro and its transformation into an excitable system. Nature 194:979–980

Nakae T (1976) Identification of the outer membrane protein of *E. coli* that produces transmembrane channels in reconstituted vesicle membranes. Biochem Biophys Res Commun 71(3):877–884

Neher E, Sakmann B (1976) Single channel currents recorded from the membrane of denervated muscle fibers. Nature 260:799–802

Nikaido H (1992) Porins and specific channels of bacterial outer membranes. Mol Microbiol 6(4):435–442

Nikaido H (2003) Molecular basis of bacterial outer membrane permeability revisited. Microbiol Mol Biol Rev 67(4):593–656

Sakmann B, Neher E (1995) Single channel recording, Second edn. Plenum, New York

Sattelle DB (ed) (1993) Planar lipid bilayers-methods and applications. Biological techniques series. Academic Press Harcourt Brace and Company, New York

Schirmer T (1998) General and specific porins from bacterial outer membranes. J Struct Biol 121:101–109

Schirmer T, Keller TA, Wang YF, Rosenbusch JP (1995) Structural basis for sugar translocation through maltoporin channels at 3.1 Å resolution. Science 267:512–514

Schulz GE (2000) Beta-barrel membrane proteins. Curr Opin Struct Biol 10:443–447

Severi E, Hood DW, Thomas GH (2007) Sialic acid utilization by bacterial pathogens. Microbiology 153:2817–2822

Teorell T (1953) Transport processes and electrical phenomena in ionic membrane. Prog Biophys Mol Biol 3:305–369

Tien HT, Ottova-Lietmannova A (eds) (2003) Membrane science and technology series. Planar lipid bilayers (BLMs) and their applications, vol 7. Elsevier, Amsterdam

Vimr ER, Kalivoda KA LDE, Steenbergen SM (2004) Diversity of microbial sialic acid metabolism. Microbiol and Mol Bio Rev 68(1):132–153

Vrouenraets M, Wierenga J, Meijberg W, Miedema H (2006) Chemical modification of the bacterial porin OmpF: gain of selectivity by volume reduction. Biophys J 90(4):1202–1211

Walker JL Jr, Eisenman G (1966) A test of the theory of the steady state properties of a liquid ion exchange membrane. Ann NY Acad Sci 137(2):777–791

Wandersman C, Schwartz M (1982) Mutations that alter the transport function of the LamB protein in Escherichia coli. J Bacteriol 151(1):15–21

Wirth C, Condemine G, Boiteux C, Berneche S, Schirmer T, Peneff CM (2009) NanC crystal structure, a model for outer-membrane channels of the acidic sugar-specific KdgM porin family. J Mol Biol 394(4):718–731. doi:10.1016/j.jmb.2009.09.054

Yamamoto D, Suzuki N (1987) Blockage of chloride channels by HEPES buffer. Proc Roy Soc B 230(1258):93–100